

Article

Selective Mineralization and Recovery of Au(III) from Multi-Ionic Aqueous Systems by *Bacillus licheniformis* FZUL-63

Yangjian Cheng ¹, Zhibin Ke ¹, Xiaojing Bian ¹, Jianhua Zhang ^{1,2}, Zhen Huang ¹, Yuancai Lv ^{1,*} and Minghua Liu ^{1,*}

¹ Fujian Provincial Engineering Research Center for High-Value Utilization Technology of Plant Resources, College of Environment & Resources, Fuzhou University, Fuzhou 350108, China

² Department of Environmental Engineering, Fujian Radiation Environmental Supervision Station, Fuzhou 350003, China

* Correspondence: yclv@fzu.edu.cn (Y.L.); mhliu2000@fzu.edu.cn (M.L.)

Received: 25 April 2019; Accepted: 25 June 2019; Published: 28 June 2019



Abstract: The recovery of precious metals is a project with both economic and environmental significance. In this paper, how to use bacterial mineralization to selectively recover gold from multi-ionic aqueous systems is presented. The *Bacillus licheniformis* FZUL-63, isolated from a landscape lake in Fuzhou University, was shown to selectively mineralize and precipitate gold from coexisting ions in aqueous solution. The removal of Au(III) almost happened in the first hour. Scanning electron microscope with X-ray energy dispersive spectroscopy (SEM/EDS-mapping) results and fourier transform infrared spectroscopy (FTIR) data show that the amino, carboxyl, and phosphate groups on the surface of the bacteria are related to the adsorption of gold ions. X-ray photoelectron spectroscopy (XPS) results implied that Au(III) ions were reduced to those that were monovalent, and the Au(I) was then adsorbed on the bacterial surface at the beginning stage (in the first hour). X-ray diffraction (XRD) results showed that the gold biomineralization began about 10 h after the interaction between Au(III) ions and bacteria. Au(III) mineralization has rarely been influenced by other co-existing metal ions. Transmission electron microscope (TEM) analysis shows that the gold nanoparticles have a polyhedral structure with a particle size of ~20 nm. The *Bacillus licheniformis* FZUL-63 could selectively mineralize and recover 478 mg/g (dry biomass) gold from aqua regia-based metal wastewater through four cycles. This could be of great potential in practical applications.

Keywords: selective biomineralization; recovery of Au(III); AuNP; *Bacillus licheniformis* FZUL-63; aqua regia-based metal wastewater

1. Introduction

Gold is a rare and precious metal that is widely used in various manufacturing industries, such as those of smart phones, personal computers (PCs), and other electrical printed circuit boards (PCBs) based electronic devices due to its excellent physical and chemical properties, electrical properties, high catalytic activity, and strong coordination ability [1–3]. However, huge amounts of electronic scraps are also generated because of the technological innovations and subsequent short lifetime of electronic devices [4,5]. PCBs are the key components and are considered the most valuable parts among electric and electronic equipment, since they contain precious metals at higher concentrations than natural high-grade ores. For example, PCBs used in smart phones and PCs contain gold with about 280 g/ton waste, which is very high compared to the 3–5 g/ton of gold in naturally occurring gold ores [5,6]. In addition, natural occurrences of these precious metals are limited and, in some mines,

already depleted. Hence, to meet the increasing demand for gold, the separation and recovery of gold from PCBs must be undertaken. The recovery of precious metals like gold from secondary sources is quite important from economic and environmental points of view [4,7].

Conventional methods such as precipitation, ion exchange, solvent extraction, and flotation for gold recovery are available, but these methods have major disadvantages, like the use of toxic chemicals, high reagent requirements, and the generation of toxic secondary waste that requires disposal [8–11]. Various biomasses have been used as biosorbents for the recovery of precious metals, such as chitosan [12], proteins [13], eggshell membranes [14], and so on, but they have major limitations in terms of their low adsorption capacity, selectivity, and reusability [15–18].

Bio-mineralization is a natural phenomenon and the process by which living organisms produce minerals. Bacterial mineralization is generally selective for elements [19–21]. For example, magnetotactic bacteria synthesize magnetosomes by selectively absorbing iron ions in the surroundings [22,23]. Bacterial mineralization used to recover metals has gained a lot of attention because of its moderate reaction conditions, lack of toxic chemicals, and good metal selectivity [24–26]. It has been reported that *Cupriavidus metallidurans* is responsible for the formation of secondary gold nano-minerals in a periplasmic space, indicating that the production of secondary gold nano-minerals may be concerned with cell active reduction [27]. However, *Delftia acidovorans* induce gold ion mineralization by secreting delftibactin (a small molecule peptide) in solution [20]. Apart from the biological accumulation of Au nanoparticles (AuNPs) in prokaryotes, eukaryotes have also been reported to form gold nano-particles by biomineralization [26,28,29].

The development of a low-cost and eco-friendly method for the recovery of gold from multi-ionic aqueous systems via bacterial biosorption and bioreduction has gained a great deal of attention [15]. Recently, a number of researches on biosynthesis of gold nanoparticles by bacteria have indicated that the synthesized nanoparticles were stable and with controllable morphology [30]. *Bacillus licheniformis* has been studied for biosynthesis of gold nanocubes, which might apply in the field of biomedicine [31]. However, the mechanisms of such a process are still poorly understood. In this paper, the *Bacillus licheniformis* FZUL-63, isolated from a landscape lake in Fuzhou University, was shown to selectively mineralize and precipitate gold, and it was used to investigate the mechanisms of the bacteria-Au interactions process, as well as its selective adsorption and reduction of gold from coexisting ions in aqueous solution. Results showed that this bacterium could be of great potential in recovering Au(III) from multi-ionic aqueous systems.

2. Materials and Methods

2.1. Microorganisms and Growth Conditions

The strain FZUL-63, isolated from a landscape lake in Fuzhou University, Fuzhou, China (GPS location: 22°03'41" N, 119°11'23" E), was identified through 16S rDNA sequence homology analysis based on the standard procedure [32]. The strain FZUL-63 was cultivated in Luria-Bertani (LB) medium with 1% Tryptone, 0.5% yeast, and 1% NaCl for 2 d at 30 °C. The cells were collected via centrifugation at 9000 rpm for 10 min and the pellet was washed with 0.9% NaCl three times, and the cells were then resuspended in the 0.9% NaCl for variation analysis. In order to prevent the formation of silver chloride precipitation, we used purified water instead of 0.9% NaCl to wash and re-suspend the cells that were acting with silver.

2.2. Metal Ion Solution and Analysis

All the chemicals used in this work were of analytical grade and were obtained from Sigma-Aldrich or Aladdin Industrial Corporation. Reagent grade water with a specific resistance of 18.2 MΩ·cm was obtained from a Milli-Q water purification system. The stock solutions (1000 mg/L) of Au(III), Cu(II), Pt(III), Cr(VI), Pb(II), Ag(I), and Zn(II) used in the experiments were prepared by dissolving HAuCl₄·3H₂O, CuSO₄·5H₂O, HPtCl₄, K₂Cr₂O₇, PbNO₃, AgNO₃, and ZnSO₄·7H₂O in purified water,

respectively. The standard solutions ranging from 1 to 200 mg/L of the metal ions were prepared by diluting the stock solutions. Adjustment of pH was carried out using 0.1 mol/L NaOH or 0.1 mol/L HNO₃. The concentration of the metal ions was measured by inductively coupled plasma optical emission spectrometry (ICP-OES) (Optima 7000 DV, PerkinElmer, Waltham, MA, USA).

2.3. Au(III) Uptake and Mineralization Experiments

The harvested and washed bacterial cells were transferred into a 100 mL Erlenmeyer flask containing 30 mL Au(III) solution (200 mg/L). The bacterial concentration was 0.05 mg/mL (dry weight) and the pH was maintained at 7 in the initial stage of the experiment. No nutrients were added to the reactors. Subsequently, the Erlenmeyer flask was incubated at 30 °C with a constant shaking speed of 160 rpm. Subsamples were collected at predetermined times and centrifuged at 5400 g for 10 min. The supernatant samples were filtered through 0.22 µm filters to remove Au(III) adsorbed on cell fragments. The residual Au(III) concentration in aqueous solution was determined by ICP-OES. All experiments were performed in triplicate.

The precipitates were freeze-dried and ground to powder in a mortar. The powder samples were analyzed by XRD (MiniFlex600, Rigaku, Japan) with CuKα ($\lambda = 0.154$ nm), an incident beam monochromator, and power of 40 kV × 20 mA [33]. Diffractograms were obtained over a 2θ range of 5 to 80° at a speed of 2°/min. Peak identification was achieved with a standard profile fitting routine provided by Philips Netherlands. Qualitative identification of mineral phases was conducted utilizing the MDI Jade 7 software [34]. The average size of the metal gold particles was calculated by the Sherrer procedure.

TEM/EDS were employed to observe the distributions of gold on the bacteria cells. After the complete interaction of Au(III) (24 h of incubation), a 2 mL cell Au(III) suspension was taken from the 200 mg/L Au(III) bio-removal experiment and centrifuged at 5400 g for 10 min. The resulting cell pellet was washed three times with deionized water. JEOL JEM-2100 LaB6 TEM (JEOL, Peabody, MA, USA) with an accelerating voltage of 200 keV fitted with STEM/EDS was employed for high-resolution imaging and for compositional analysis. To identify the reduced gold mineral, the selected area electron diffraction (SAED) pattern was acquired with a Gatan Orius SC200D camera [35].

SEM and elemental mapping were employed to observe the distributions of gold on the bacteria cells. SEM observations were made to identify any morphological changes of *B. licheniformis* upon the exposure of Au(III) and to identify any mineral phase formed from Au(III) adsorption. Among the different Au(III) concentrations used for the adsorption experiment, the 200 mg/L Au(III) sample was observed under SEM. Cells were first fixed for 20 min with 2% formaldehyde and 2.5% glutaraldehyde in a 0.05 mol/L sodium cacodylate buffer (pH 7.2) at a 1:1 ratio (sample: fixative). After this primary fixation, a few drops of sample suspension were placed over the surface of a glass cover slip and sequentially dehydrated using varying proportions of ethanol followed by critical point drying with a Tousimis Samdri-780A (Tousimis Research Corp., Rockville, MD, USA) critical point dryer (CPD). Critical point dried samples were coated with carbon using a Denton vacuum evaporator DV-502A (Denton Vacuum Inc., Moorestown, NJ, USA). A Zeiss Supra 35 VP SEM (Carl Zeiss, Jena, Germany) with Genesis 2000 X-ray energy-dispersive spectroscopy (SEM/EDS) was employed for cell imaging and compositional analyses.

2.4. X-ray Photoelectron Spectroscopy (XPS) Analysis

The chemical states of gold in the samples were measured by XPS. The powder samples of bacteria reacting with Au(III) for different times were placed in an evacuated sample chamber. Survey spectra were collected over the range of 0–1200 eV with a pass energy of 30.0 eV. High-resolution XPS spectra were acquired for C1s [36]. All binding energy values were calibrated by using the value of contaminant carbon (284.65 eV) as a reference [37]. The spectra for Au were obtained under conditions of 0.05 eV steps and analyzed after corrections.

2.5. Selective Mineralization Experiments

The common metal ions in electroplating wastewater include Au(III), Cu(II), Pt(III), Cr(VI), Pb(II), Ag(I), Zn(II), and so on. The above-mentioned ions were prepared in every 100 mL Erlenmeyer flask by diluting the stock solution, respectively. The gold stock solution was added to the various Erlenmeyer flasks with the initial concentration of 200 mg/L, except for the Erlenmeyer flask containing the Ag(I) solution, as Ag(I) ions cannot coexist with the $\text{HAuCl}_4 \cdot 3\text{H}_2\text{O}$ solution. After adding the Au(III), the initial concentrations of Cu(II), Pt(III), Cr(VI), Pb(II), Ag(I), and Zn(II) were adjusted to 200 mg/L and the bacterial dosage was 1 g dry weight per liter in each 100 mL Erlenmeyer flask containing the 25 mL solution. Subsequently, the Erlenmeyer flasks were incubated at 30 °C with a constant shaking speed of 160 rpm. Subsamples were collected at predetermined times and centrifuged at 5400 g for 10 min. The residual ion concentrations in the supernatant were determined by ICP-OES and the pellets were analyzed by XRD and TEM, as mentioned above.

2.6. Recovery of Au(III) From Aqua Regia-Based Metal Wastewater

As much other metal as possible was removed, except for gold ions from PCBs with nitric acid, the insoluble substance was collected and treated with aqua regia. Then, the pH was adjusted to 6.0 with 5 mol/L KOH and centrifuged. The metal ion concentrations in the supernatant, also called the aqua regia-based metal wastewater, were determined by ICP-OES, as mentioned above.

The bacteria were added to the supernatant with the amount of 1 g of biomass (dry weight) per liter. Subsequently, the Erlenmeyer flasks were incubated at 30 °C with a constant shaking speed of 160 rpm. Subsamples were collected at predetermined times for analysis. In the reaction platform stage, bacteria and gold nanoparticles were collected by centrifugation at 5400 g for 10 min, and the aqua regia-based metal wastewater was added to the collection containing bacteria and gold nanoparticles again. This was then cycled many times until the bacteria had less or no ability to mineralize Au(III).

3. Results and Discussion

3.1. Au(III) Uptake and Mineralization

The strain FZUL-63 was identified as *Bacillus licheniformis* through 16S rDNA sequence homology analysis. *B. licheniformis* removed Au(III) from aqueous solution as a function of time. *B. licheniformis* removed Au(III) from aqueous solution as a function of time, as shown in the graph of Figure 1a. In this process, the color of the culture in the Erlenmeyer flask turns from bright yellow to pink (10 h), and finally becomes wine red (Figure 1a), which was attributed to the formation of AuNPs. It is reported that gold nanoparticles show different colors according to different sizes (the bigger the particle size, the darker the color) [38]. The solid phase samples collected from different interaction times were analyzed by XRD (Figure 1b). In the first hour, no peaks were detected in XRD patterns after the interaction between bacteria and Au(III), suggesting that adsorbed Au(III) did not form crystalline phases. Although no crystalline phases were detected with XRD after a 1 h interaction, with a prolonged time, some weak peaks were observed in the XRD pattern after 10 hours of interaction, implying that a small amount of gold mineral formed (Figure 1b). The newly observed diffraction peaks matched well with gold. These results suggest that with time, the bacterium may have mediated Au(III) transformation from an amorphous compound to stable AuNPs. Under TEM, there were many AuNPs with a ~20 nm grain size on and around the bacterial cell surface (Figure 1a). It was reported that bacterial metabolic activity might be inhibited by the toxicity of Au [20]. However, our colony counting experiments showed that after 30 h of interaction with Au, the number of viable cells was not significantly reduced (before interaction: 3.6×10^8 CFU/mL; after interaction: 2.9×10^8 CFU/mL). Therefore, the cell metabolic activity might play a vital role in Au adsorption and mineralization process.

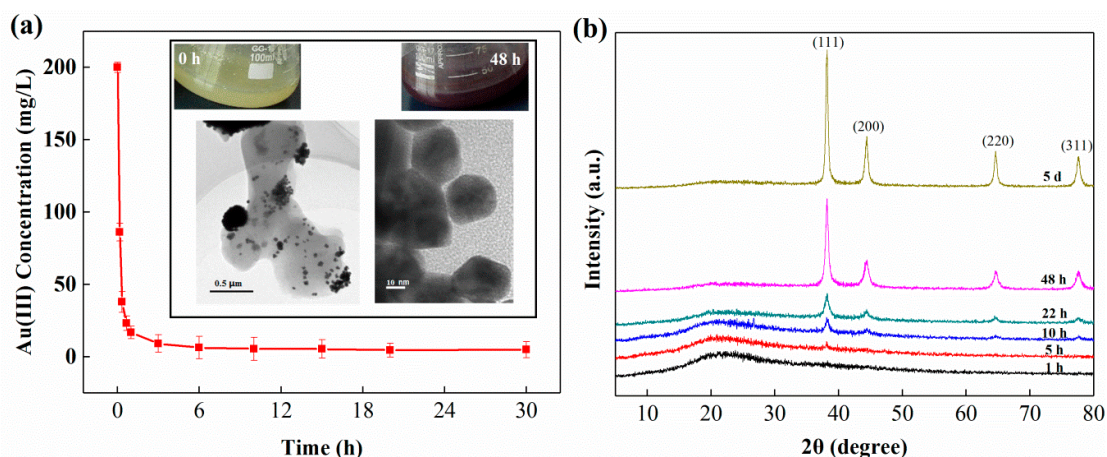


Figure 1. The interaction between bacteria and Au(III) with time. (a) The Au(III) concentration in aqueous solution. The inserts show the color of the culture (top) at 0 h and 48 h, respectively; and TEM images of cells and Au particles (bottom) at 48 h. (b) XRD pattern of the AuNPs enhanced over time.

3.2. The Chemical Groups Involved in Gold Binding

The gold ions in the aqueous solution were quickly removed (Figure 1a), but the XRD results indicate that no minerals formed in the initial stage (Figure 1b), so the gold ions may have been adsorbed on the surface of the bacteria first. SEM/EDS-mapping was conducted to investigate spatial association between Au and C, O, N, P, S in the bacterial surface. As shown in Figure 2c,d, Au detected in the bacterial surface and was co-localized with C, O, N, P, S, indicating involvements of functional groups which contain these elements during adsorption process.

To further elucidate the chemical groups involved in gold binding, FTIR spectra were recorded for control and gold-loaded cells from 4000 cm^{-1} to 400 cm^{-1} (Figure 2). The characteristic peaks can be assigned to the involvement of the main functional groups present in the bacterial biomass by analyzing the highly complex IR spectra (Figure 2h). The N–H stretching peak that lies in the spectrum region occupied by a broad and strong band in the $3200\text{--}3600\text{ cm}^{-1}$ region was due to the presence of $\gamma\text{O–H}$ of the hydroxyl groups, which undergo change in the peak position in the gold loaded spectrum, suggesting the involvement of amino and hydroxyl groups in gold binding to the bacterial surface [39,40]. In the spectra for gold-loaded cells, the peak around 2366 cm^{-1} could be assigned to the P–O stretching vibrations, implying a possible role of phosphate metabolism, facilitating the cellular adsorption of gold ions. The spectra for both control and gold-loaded samples revealed protein-related bands. The appearance of $\gamma\text{C=O}$ of amide I and the $\delta\text{NH}/\gamma\text{C=O}$ combination of the amide II bonds that were present at 1652 cm^{-1} and 1543 cm^{-1} , respectively, were predominant in the control spectrum. Following Au binding, the amide I absorption peak (1652 cm^{-1}) was split into two minor peaks at 1664 cm^{-1} and 1639 cm^{-1} and a marked shift of the 1543 cm^{-1} peak to 1541 cm^{-1} suggests the interaction of Au with carboxyl groups. In the control spectrum, sharp peaks between 1400 cm^{-1} and 1500 cm^{-1} were due to the presence of the carboxyl groups [31]. Particularly, the strong peak at 1451 cm^{-1} , which was characteristic of the scissoring motion of CH_2 groups [32], underwent a shift to a lower energy level (1449 cm^{-1}) after gold binding. Following gold uptake, a clear shift of the peak at 1399 cm^{-1} to 1388 cm^{-1} due to the symmetric stretching of COO^- vibration strongly indicated a role of carboxyl groups in gold binding [40]. In the control spectrum, the strong peaks at 1238 cm^{-1} and 1062 cm^{-1} were observed due to vibrations of carboxyl and phosphate groups [41]. Following gold exposure, a clear shift of these peaks to 1234 cm^{-1} and 1057 cm^{-1} suggests the interaction of bound metals with carboxyl and phosphate groups. A gradual shift of the peak in control spectra at 1238 cm^{-1} , because of asymmetric stretching modes of protonated polyphosphates and PO uncomplexed in phosphate diesters to 1234 cm^{-1} in gold-loaded samples, indicated the weakening of the P=O character as a result of metal binding to the phosphates [41]. Changes in the peak position and intensity in the 800 cm^{-1} to

400 cm^{-1} region could be assigned to the formation of intense (M–O) and (O–M–O) bonds (M = metal ion) [39]. The overall IR spectroscopic analysis suggests that phosphate, carboxyl, and amide groups on bacterial cells are the dominant functional groups involved in the bacteria-gold interaction.

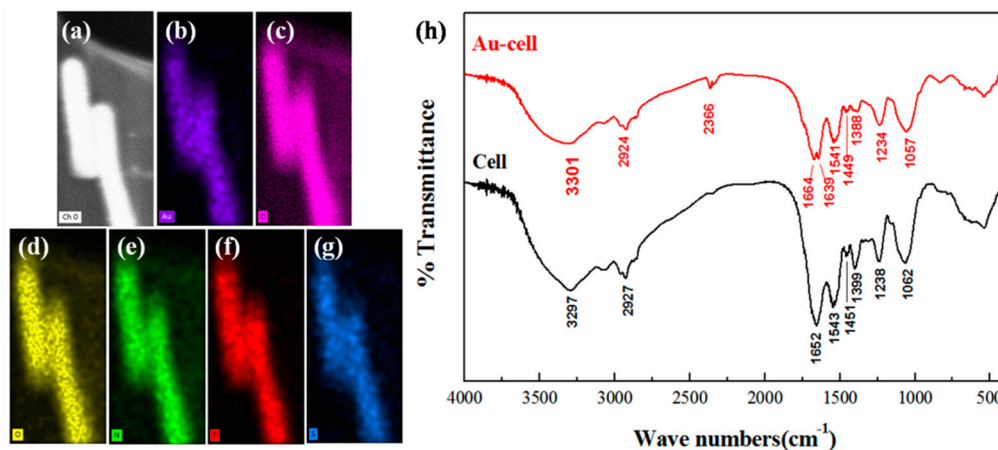


Figure 2. (a) SEM image of *B. licheniformis* FZUL-63 after interaction with gold; (b–g) elemental maps of Au, C, O, N, P, and S, respectively; (h) Fourier transformed infrared spectra of *B. licheniformis* FZUL-63 biomass: before and after gold uptake (initial concentration of 200 $\text{mg Au (III) L}^{-1}$ at pH 6.0, time 1 h).

3.3. Changes in the Chemical Valence State of Gold

The interaction of Au(III) with bacteria at different times has been investigated by XPS. The Au 4f spectra of all the investigated samples are shown in Figure 3. The evidence is confirmed by the curve-fitting of the Au 4f core-level spectra by two spin-orbit split Au 4f_{7/2} and Au 4f_{5/2} components (DE~4.0 eV), showing increasing BE values that correspond to a different chemical state of gold particles in the samples. With the initial addition of the chloric acid sample, the Au 4f_{7/2} photoelectronic peak is located at BE = 84.38 eV and this value is typical of Au(III) species, Figure 3a. After the interaction of the trivalent gold ions with bacteria, in the one-hour sample, shown in Figure 3b, the Au 4f_{7/2} spectrum consists of only one component located at BE = 84.80 eV, which can be assigned to Au(I) species. In the 48-hour sample, the Au 4f_{7/2} peak detected at BE = 83.81 eV shown in Figure 3c can be attributed to the presence of Au(0) species on the bacterial surface. From the changes in the valence state after the action of trivalent gold ions and bacteria, it could be deduced that trivalent gold ions are not reduced to zero-valent gold (AuNP) in one step and the intermediates of monovalent gold compounds were produced in the reduced process.

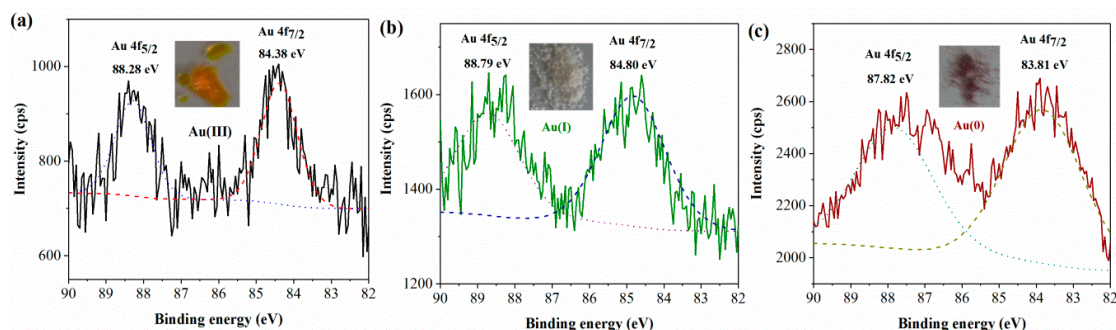


Figure 3. XPS spectra of the Au(4f) region of interaction with bacteria for (a) 0 h; (b) 1 h; and (c) 48 h.

3.4. Coexisting Ions Affect the Mineralization and Recovery of Gold

The aqua regia-based metal wastewater usually contains the following metal ions: Au(III), Pt(III), Ag(I), Cr(VI), Pb(II), Zn(II), and Cu(II). The chloroauric acid and the silver ion cannot coexist in the

solution. Therefore, we only conducted experiments using gold and silver acting alone with bacteria, and their recovery percentages were 97.66% and 49.23%, respectively (Figure 4a). The 200 mg/L Cr(VI) ions could delay the recovery balance time of the gold from one hour to 18 h, and the recovery percentage of gold was also reduced from 97.66% to 91.93% (Figure 4b). Zn(II) and Cu(II) rarely influenced the Au(III) recovery (Figure 4c,d). However, for the 200 mg/L Pt(III) or Pb(II) coexisting with Au(III), the recovery percentage of gold was reduced from 97.66% to 85.06% and 93.31%, respectively (Figure 4e,f).

On the contrary, when these ions coexisted with the gold ions, the gold ions could preferentially adsorb on bacterial surface, leading to reducing adsorption of other ions. The removal percentage Pt and Pb ions have obvious reduction (Figure 4c,d). Compared with the removal percentage of Pt(III) and Pb(II) via bacteria alone, the removal percentage of Pt(III) and Pb(II) decreased from 45.82% to less than 0.5% and 56% to 17.33% in the presence of gold ions, respectively. The results indicated that *B. licheniformis* was able to preferentially adsorb and reduce Au(III) to Au(0) from multi ionic aqueous system. The reason for preferential adsorption and reduction might be the following two aspects: one is the cell metabolic activity; the other is the redox potential orders of metals.

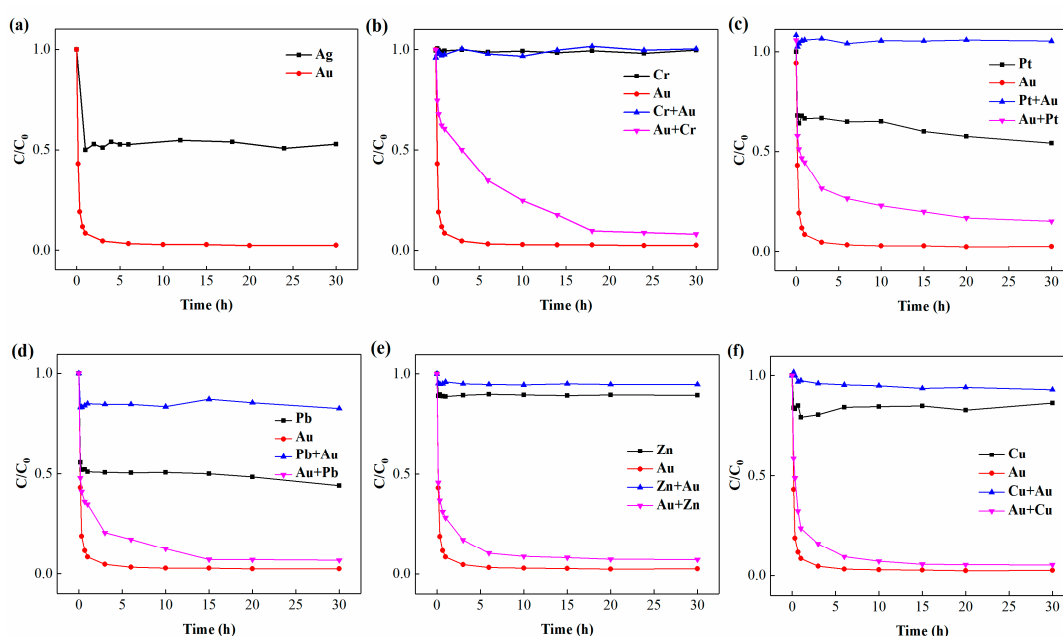


Figure 4. Au(III) recovery influenced by coexisting metal ions. (a) using gold and silver acting alone with bacteria. (b–f) using gold and other metal acting together with the bacteria. The initial concentration of each ion is 200 mg/L, and the bacterial dosage is 1 g dry weight per liter. “Au + other metal” represent Au concentration while “other metal + Au” is the concentration of other metal in the mixed solution.

3.5. Recovery of Au(III) Form Metal Wastewater

The PCBs were treated with strong nitric acid. The insoluble substance was collected by centrifugation and treated with aqua regia. It was then adjusted to a pH of 6.0 and centrifuged. The concentration of ions in the supernatant was measured by ICP-OES, and the concentration of each ion before and after bacterial treatment is shown in Table 1.

Table 1. Recovery of Au (III) from aqua regia-based metal wastewater in the first cycle.

Metal Concentration (mg/L)	Au ³⁺	Cu ²⁺	Zn ²⁺	Pb ²⁺	Pt ⁴⁺	Cr ⁶⁺	Fe ³⁺	Ni ²⁺	Ag ⁺
Without cell	181.2 ± 3.2	348.5 ± 3.7	120.0 ± 2.3	39.2 ± 2.6	16.1 ± 1.1	27.3 ± 2.4	85.4 ± 3.5	48.7 ± 2.9	ND
With cell	17.4 ± 1.2	330.7 ± 2.5	115.2 ± 2.2	34.3 ± 1.7	15.9 ± 1.3	26.1 ± 1.9	80.6 ± 3.1	47.3 ± 2.7	ND
Removal efficiency (%)	90.4%	5.1%	4.0%	12.5%	1.3%	4.4%	5.6%	2.9%	–

Note: ND indicates that the concentration is below the limit of detection. All experiments were performed in triplicate.

As Figure 5 shows, through the first treatment, the recovery percentage of gold was 90.4%. After the second treatment, the gold recovery percentage dropped to 82.3%. The gold recovery percentages were 61.8% and 29.6% at the third and fourth treatment, respectively. AuNPs could be recovered by acid dissolution. For example, the bacteria and gold nanoparticles were collected by centrifugation at 5400 g for 10 min and treated with 1 mol/L HCl, which may dissolve the bacterial cells. Then, the acid dissolution sample was centrifuged at low rotation speed (2000 rpm for 20 min) to remove supernatant containing cell debris, DNA and so on. The pellet was gold particles with high purity. With four cycles, we could recover 478 mg of AuNPs per gram of bacteria from the aqua regia-based metal wastewater.

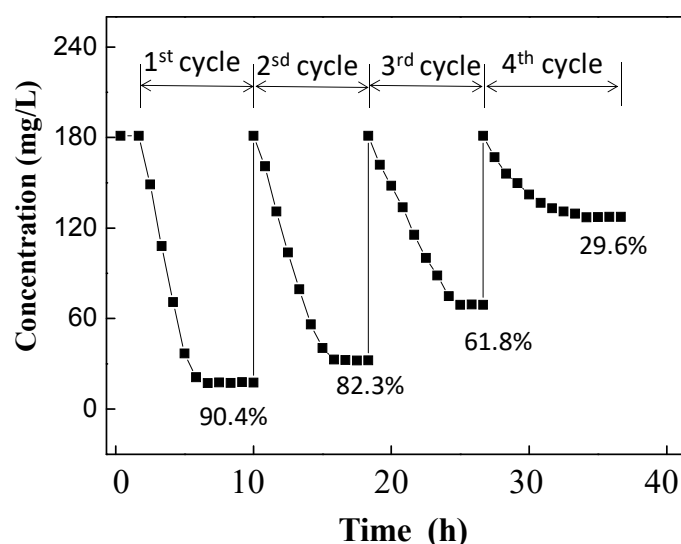


Figure 5. The *Bacillus licheniformis* FZUL-63 selectively mineralizes and recovers gold from aqua regia-based metal wastewater through four cycles.

4. Conclusions

An indigenous bacterium *Bacillus licheniformis* FZUL-63 was shown to selectively mineralize and precipitate gold from coexisting ions in aqueous solution. The process is as follows: Au(III) ions are reduced to those that are monovalent by the *B. licheniformis*, and the Au(I) is then adsorbed on the bacterial surface in the beginning stage. The amino, carboxyl, and phosphate groups on the surface of the bacteria are related to the adsorption of gold ions. The gold biomineralization has rarely been influenced by other co-existing metal ions. The bacteria could recover 478 mg/g (dry biomass) of gold from aqua regia-based metal wastewater through four cycles.

Author Contributions: Conceptualization, Y.C.; methodology, H.Z.; investigation, X.B.; resources, J.Z.; data curation, Z.K.; writing—original draft preparation, X.B.; writing—review and editing, Y.C.; project administration, Y.L.; funding acquisition, M.L.

Funding: This work was financially supported by the National Basic Research Program of China (973 Program) (no. 2014CB846003), the National Natural Science Foundation of China (no. 41372346, 21477129), and the Natural Science Foundation of Fujian Province (no. 2019J01246). Additional support was provided by the China Scholarship Council (no. 201506655045) and the CSC-DAAD PPP Programmes for Project-Related Personal

Exchange (no. 2019-12039). The funders had no role in the design of the study; in the collection, analyses, or interpretation of data; in the writing of the manuscript, or in the decision to publish the results.

Conflicts of Interest: The authors declare no conflict of interest.

References

1. Yin, P.; Xu, M.Y.; Qu, R.J.; Chen, H.; Liu, X.G.; Zhang, J.; Xu, Q. Uptake of gold (III) from waste gold solution onto biomass-based adsorbents organophosphonic acid functionalized spent buckwheat hulls. *Bioresour. Technol.* **2013**, *128*, 36–43. [[CrossRef](#)]
2. Fan, R.Y.; Xie, F.; Guan, X.L.; Zhang, Q.L.; Luo, Z.R. Selective adsorption and recovery of Au(III) from three kinds of acidic systems by persimmon residual based bio-sorbent: A method for gold recycling from e-wastes. *Bioresour. Technol.* **2014**, *163*, 167–171. [[CrossRef](#)]
3. Kwak, I.S.; Yun, Y.S. Recovery of zero-valent gold from cyanide solution by a combined method of biosorption and incineration. *Bioresour. Technol.* **2010**, *101*, 8587–8592. [[CrossRef](#)]
4. Hyder, M.; Ochiai, B. Selective recovery of Au(III), Pd(II), and Ag(I) from printed circuit boards using cellulose filter paper grafted with polymer chains bearing thiocarbamate moieties. *Microsyst. Technol.* **2018**, *24*, 683–690. [[CrossRef](#)]
5. Choudhary, B.C.; Paul, D.; Borse, A.U.; Garole, D.J. Surface functionalized biomass for adsorption and recovery of gold from electronic scrap and refinery wastewater. *Sep. Purif. Technol.* **2018**, *195*, 260–270. [[CrossRef](#)]
6. Van Eygen, E.; De Meester, S.; Tran, H.P.; Dewulf, J. Resource savings by urban mining: The case of desktop and laptop computers in Belgium. *Resour. Conserv. Recy.* **2016**, *107*, 53–64. [[CrossRef](#)]
7. Syed, S. Recovery of gold from secondary sources—A review. *Hydrometallurgy* **2012**, *115*, 30–51. [[CrossRef](#)]
8. Sheel, A.; Pant, D. Recovery of gold from electronic waste using chemical assisted microbial biosorption (hybrid) technique. *Bioresour. Technol.* **2018**, *247*, 1189–1192. [[CrossRef](#)]
9. Alzate, A.; Lopez, M.E.; Serna, C. Recovery of gold from waste electrical and electronic equipment (WEEE) using ammonium persulfate. *Waste Manag.* **2016**, *57*, 113–120. [[CrossRef](#)]
10. Natarajan, G.; Ting, Y.P. Gold biorecovery from e-waste: An improved strategy through spent medium leaching with pH modification. *Chemosphere* **2015**, *136*, 232–238. [[CrossRef](#)]
11. Yap, C.Y.; Mohamed, N. An electrogenerative process for the recovery of gold from cyanide solutions. *Chemosphere* **2007**, *67*, 1502–1510. [[CrossRef](#)]
12. Zhang, M.; Zhang, Y.; Helleur, R. Selective adsorption of Ag⁺ by ion-imprinted O-carboxymethyl chitosan beads grafted with thiourea-glutaraldehyde. *Chem. Eng. J.* **2015**, *264*, 56–65. [[CrossRef](#)]
13. Maruyama, T.; Matsushita, H.; Shimada, Y.; Kamata, I.; Hanaki, M.; Sonokawa, S.; Kamiya, N.; Goto, M. Proteins and protein-rich biomass as environmentally friendly adsorbents selective for precious metal ions. *Environ. Sci. Technol.* **2007**, *41*, 1359–1364. [[CrossRef](#)]
14. Devi, P.S.; Banerjee, S.; Chowdhury, S.R.; Kumar, G.S. Eggshell membrane: A natural biotemplate to synthesize fluorescent gold nanoparticles. *Rsc. Adv.* **2012**, *2*, 11578–11585. [[CrossRef](#)]
15. Ju, X.H.; Igarashi, K.; Miyashita, S.; Mitsushashi, H.; Inagaki, K.; Fujii, S.I.; Sawada, H.; Kuwabara, T.; Minoda, A. Effective and selective recovery of gold and palladium ions from metal wastewater using a sulfothermophilic red alga, *Galdieria sulphuraria*. *Bioresour. Technol.* **2016**, *211*, 759–764. [[CrossRef](#)]
16. Kaksonen, A.H.; Mudunuru, B.M.; Hackl, R. The role of microorganisms in gold processing and recovery—A review. *Hydrometallurgy* **2014**, *142*, 70–83. [[CrossRef](#)]
17. Das, N. Recovery of precious metals through biosorption—A review. *Hydrometallurgy* **2010**, *103*, 180–189. [[CrossRef](#)]
18. Zhang, T.; Tu, Z.H.; Lu, G.N.; Duan, X.C.; Yi, X.Y.; Guo, C.L.; Dang, Z. Removal of heavy metals from acid mine drainage using chicken eggshells in column mode. *J. Environ. Manag.* **2017**, *188*, 1–8. [[CrossRef](#)]
19. Malhotra, A.; Dolma, K.; Kaur, N.; Rathore, Y.S.; Ashish; Mayilraj, S.; Choudhury, A.R. Biosynthesis of gold and silver nanoparticles using a novel marine strain of *Stenotrophomonas*. *Bioresour. Technol.* **2013**, *142*, 727–731. [[CrossRef](#)]
20. Johnston, C.W.; Wyatt, M.A.; Li, X.; Ibrahim, A.; Shuster, J.; Southam, G.; Magarvey, N.A. Gold biomineralization by a metallophore from a gold-associated microbe. *Nat. Chem. Biol.* **2013**, *9*, 241–243. [[CrossRef](#)]

21. Nita, R.; Trammell, S.A.; Ellis, G.A.; Moore, M.H.; Soto, C.M.; Leary, D.H.; Fontana, J.; Talebzadeh, S.F.; Knight, D.A. Kinetic analysis of the hydrolysis of methyl parathion using citrate-stabilized 10 nm gold nanoparticles. *Chemosphere* **2016**, *144*, 1916–1919. [[CrossRef](#)]
22. Uebe, R.; Schuler, D. Magnetosome biogenesis in magnetotactic bacteria. *Nat. Rev. Microbiol.* **2016**, *14*, 621–637. [[CrossRef](#)]
23. Amor, M.; Busigny, V.; Louvat, P.; Gelabert, A.; Cartigny, P.; Durand-Dubief, M.; Ona-Nguema, G.; Alphantery, E.; Chebbi, I.; Guyot, F. Mass-dependent and -independent signature of Fe isotopes in magnetotactic bacteria. *Science* **2016**, *352*, 705–708. [[CrossRef](#)]
24. Lu, A.H.; Li, Y.; Jin, S. Interactions between semiconducting minerals and bacteria under light. *Elements* **2012**, *8*, 125–130. [[CrossRef](#)]
25. Pavlova, L.M.; Radomskaya, V.I. Biomineralization of precious metals. *Biog. Abiogenic Interact. Nat. Anthropog. Syst.* **2016**, 15–27.
26. Narayanan, K.B.; Park, H.H.; Han, S.S. Synthesis and characterization of biomatrixed-gold nanoparticles by the mushroom *Flammulina velutipes* and its heterogeneous catalytic potential. *Chemosphere* **2015**, *141*, 169–175. [[CrossRef](#)]
27. Reith, F.; Etschmann, B.; Grosse, C.; Moors, H.; Benotmane, M.A.; Monsieurs, P.; Grass, G.; Doonan, C.; Vogt, S.; Lai, B.; et al. Mechanisms of gold biomineralization in the bacterium *Cupriavidus metallidurans*. *Natl. Acad. Sci. USA* **2009**, *106*, 17757–17762. [[CrossRef](#)]
28. Das, S.K.; Liang, J.; Schmidt, M.; Laffir, F.; Marsili, E. Biomineralization mechanism of gold by zygomycete fungi *rhizopus oryzae*. *ACS Nano*. **2012**, *6*, 6165–6173. [[CrossRef](#)]
29. Lengke, M.F.; Fleet, M.E.; Southam, G. Morphology of gold nanoparticles synthesized by filamentous cyanobacteria from gold(I)-thiosulfate and gold(III)-chloride complexes. *Langmuir* **2006**, *22*, 2780–2787. [[CrossRef](#)]
30. Shedbalkar, U.; Singh, R.; Wadhvani, S.; Gaidhani, S.; Chopade, B.A. Microbial synthesis of gold nanoparticles: Current status and future prospects. *Adv. Colloid. Interfac.* **2014**, *209*, 40–48. [[CrossRef](#)]
31. Kalishwaralal, K.; Deepak, V.; Pandian, S.R.K.; Gurunathan, S. Biological synthesis of gold nanocubes from *Bacillus licheniformis*. *Bioresour. Technol.* **2009**, *100*, 5356–5358. [[CrossRef](#)]
32. Lin, W.T.; Huang, Z.; Li, X.Z.; Liu, M.H.; Cheng, Y.J. Bio-remediation of acephate-Pb(II) compound contaminants by *Bacillus subtilis* FZUL-33. *J. Environ. Sci. China* **2016**, *45*, 94–99. [[CrossRef](#)]
33. Cheng, Y.J.; Zhang, L.; Bian, X.J. Adsorption and mineralization of REE—Lanthanum onto bacterial cell surface. *Environ. Sci. Pollut. Res.* **2017**, *25*, 22334–22339. [[CrossRef](#)]
34. Cheng, Y.J.; Xu, X.Y.; Yan, S.G.; Pan, X.H.; Chen, Z.; Lin, Z. Hydrothermal growth of large-size UO₂ nanoparticles mediated by biomass and environmental implications. *Rsc. Adv.* **2014**, *4*, 62476–62482. [[CrossRef](#)]
35. Singh, R.; Dong, H.L.; Liu, D.; Zhao, L.D.; Marts, A.R.; Farquhar, E.; Tierney, D.L.; Almquist, C.B.; Briggs, B.R. Reduction of hexavalent chromium by the thermophilic methanogen *Methanothermobacter thermoautotrophicus*. *Geochim. Cosmochim. Acta* **2015**, *148*, 442–456. [[CrossRef](#)]
36. Bao, X.Q.; Qin, Z.; Zhou, T.S.; Deng, J.J. In-situ generation of gold nanoparticles on MnO₂ nanosheets for the enhanced oxidative degradation of basic dye (Methylene Blue). *J. Environ. Sci. China* **2018**, *65*, 236–245. [[CrossRef](#)]
37. Miah, A.; Malakar, B.; Saikia, P. Gold over ceria-titania mixed oxides: Solar light induced catalytic activity for nitrophenol reduction. *Catal. Lett.* **2016**, *146*, 291–303. [[CrossRef](#)]
38. Kumar, S.A.; Peter, Y.A.; Nadeau, J.L. Facile biosynthesis, separation and conjugation of gold nanoparticles to doxorubicin. *Nanotechnology* **2008**, *19*, 495101. [[CrossRef](#)]
39. Choudhary, S.; Sar, P. Uranium biomineralization by a metal resistant *Pseudomonas aeruginosa* strain isolated from contaminated mine waste. *J. Hazard Mater.* **2011**, *186*, 336–343. [[CrossRef](#)]
40. Pagnanelli, F.; Papini, M.P.; Toro, L.; Trifoni, M.; Veglio, F. Biosorption of metal ions on *Arthrobacter* sp.: Biomass characterization and biosorption modeling. *Environ. Sci. Technol.* **2000**, *34*, 2773–2778. [[CrossRef](#)]
41. Jiang, W.; Saxena, A.; Song, B.; Ward, B.B.; Beveridge, T.J.; Myneni, S.C.B. Elucidation of functional groups on gram-positive and gram-negative bacterial surfaces using infrared spectroscopy. *Langmuir* **2004**, *20*, 11433–11442. [[CrossRef](#)]

